Publishing House
AKAPIT

COMPUTER METHODS IN MATERIALS SCIENCE

Informatyka w Technologii Materiałów

Vol. 15, 2015, No. 3

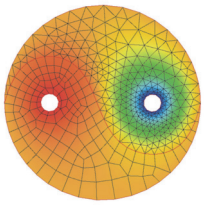

DP_BUILDER - THE COMPUTER SYSTEM FOR THE DESIGN OF THE CONTINUOUS ANNEALING CYCLES FOR DP STEELS

GRZEGORZ GÓRECKI[1]*, ROMAN KUZIAK[2], NORBERT KWIATON[3], ŁUKASZ MADEJ[1], MACIEJ PIETRZYK[1]

[1] AGH University of Science and Technology, a. Mickiewicza 30, 30-059 Kraków, Poland
[2] Institute for Ferrous Metallurgy, K. Miarki 12, 44-100 Gliwice, Poland
[3] Salzgitter Mannesmann Forschung GmbH, Eisenhüttenstraße 99, 38239 Salzgitter, Germany
**Corresponding author: ggorecki@agh.edu.pl*

Abstract

The *DP_builder* software, which was developed to design the best continuous annealing technology for DP steels in a fast and efficient way, is presented in the paper. The key components of the system, including models of phase transformations during heating and cooling stages, are described first. Following this, major principles, features and implementation details of the system are presented. Main functionalities provide possibilities of simulation of microstructure evolution during various thermal cycles and capability to design the best technological variant. Additionally a database, which stores material and technological information for all previously analyzed cases, was designed and incorporated in the system. Finally, graphical user interface was added to make the system easily accessible and user friendly.

Key words: DP steels, continuous annealing, computer system, optimal thermal cycles

1. INTRODUCTION

Continuous development of the automotive industry creates demand for metallic materials that combine high strength with good ductility. One of the possibility to fulfil the demand is application of the Advanced High Strength Steels (AHSS) that have been intensively developed for more than a decade now (Hofmann, 2009; Matlock, 2005; Matlock & Speer, 2009). Dual Phase (DP) steels belong to the most common and popular AHSSs. Due to their specific microstructure, they meet those high requirements and are currently used by the automotive industry.

The DP steel is a composite of ductile ferrite and hard martensite phases and can also contain bainite and retained austenite. The required phase fractions within the microstructure are obtained during the continuous annealing. Recrystallization of deformed ferrite and austenitizing during the continuous heating as well as phase transformation during the continuous cooling are the main processes to obtain the desired microstructure. Volume fraction of martensite or MA (martensite with small islands of the retained austenite) determine the strength of DP steel. For a DP 600 volume fraction of martensite is usually between 15 and 25%. This phase composition gives high strength and good workability, which are important properties from an automotive industry point of view.

As presented a typical continuous annealing process involves sophisticated thermal cycle, which makes manufacturing of DP steels a complex problem and requires precise control of process parameters. It is expected that numerical simulation will help to design the optimal process. Thus, development of the model, which is capable to simulate

 ISSN 1641-8581

phenomena occurring in DP steels, is important. Models of static recrystallization as well as phase transformations during heating and cooling stages of the continuous annealing process were developed and validated by Pietrzyk and Kuziak (2012) and are only briefly described in the following section. These models can evaluate various complex thermal cycles and compare them. On the other hand, large number of the design variables makes selection of the best cycle difficult. Therefore, development of the user friendly computer system based on mentioned models was the main objective of the present work. In literature lack such customised software designed to deal with the continuous annealing.

2. MICROSTRUCTURE EVOLUTION MODELS

The model should allow realistic description of phase transformations, good accuracy and reliability of calculations, as well as should provide certain special predictive capabilities. Model of phase transformations during heating and during cooling was based on the modified Avrami equation (Avrami, 1939) and is described by Pietrzyk and Kuziak (2012):

$$X = 1 - \exp\left(-kt^n\right) \tag{1}$$

where: X – volume fraction of the new phase, t – time.

It was shown by Pernach et al. (2013) that this model allows efficient simulation of the continuous annealing. Main equations of this model are repeated below.

Equation (1) is combined with the Scheil (1935) additivity rule, which accounts for the temperature variations. Theoretical considerations show that a constant value of n in equation (1) can be used for modelling ferritic, pearlitic and bainitic transformations (n_f, n_p, and n_b respectively). On the contrary, the coefficient k vary with temperature T and the formalism of the function $k = f(T)$ has to be carefully chosen to describe properly the transformation kinetics. A modified Gaussian function proposed by Donnay et al. (1996) was selected for the ferritic transformation:

$$k_f = k_m \exp\left[-\left(\frac{T - T_n}{p}\right)^q\right] \tag{2}$$

Coefficients k_m, T_n, p and q allow description of all shapes of the CCT diagram in an intuitive way. Thus, $k_m = a_1/D_\gamma$ is the maximum value of k, $T_n = A_{e3} + 400/D_\gamma - a_2$ is a position of the nose of the modified Gaussian function (2), p determines the width at mid height of this function and q controls the sharpness of the curve. D_γ is the austenite grain size prior to transformation.

The sensitivity analysis has shown that the model output is not sensitive to coefficients describing relation $k = f(T)$ for the pearlitic transformation and constant value of $k = k_p$ was assumed for this transformation. The following equation describes k for the bainitic transformation:

$$k_b = b_6 \exp\left(b_5 - 0.01 b_4 T\right) \tag{3}$$

Equation (1) with the modified Gauss function (2) describes properly nucleation, growth and site saturation mechanisms for lean chemical composition of steels. This equation accounts directly for the incubation time for the ferritic transformation. An assumption is made that transformation begins when 5% of ferrite occurs in the microstructure. Incubation time has to be introduced for pearlitic (τ_p) and bainitic (τ_b) transformations:

$$\tau_P = \frac{p_1}{\left(\mathrm{A}_{e1} - T\right)^{p_3}} \exp\left[\frac{p_2}{R\left(T + 273\right)}\right]$$

$$\tau_b = \frac{b_1}{\left(B_s - T\right)^{b_3}} \exp\left[\frac{b_2}{R\left(T + 273\right)}\right] \tag{4}$$

where: R – gas constant, B_s – bainite start temperature.

Start temperatures for the bainitic (B_s) and martensitic (M_s) transformations are given by:

$$B_s[^\circ\mathrm{C}] = b_0 - 425[\mathrm{C}] - 42.5[\mathrm{Mn}] - 31.5[\mathrm{Ni}] \tag{5}$$

$$M_s[^\circ\mathrm{C}] = m_1 - m_2 c_\gamma \tag{6}$$

where: c_γ – current carbon content in the austenite.

Fraction of austenite with respect to the whole volume of the sample is calculated as (Koistinen & Marburger, 1959):

$$F_m = \left(1 - F_f - F_p - F_b\right)\left\{1 - \exp\left[-0.011\left(M_s - T\right)\right]\right\} \tag{8}$$

where: F_f, F_p, F_b – volume fractions of ferrite, pearlite and bainite, respectively.

Two processes occur during heating stage, recrystallization of ferrite and phase transformation of the ferritic-pearlitic microstructure into austenite. In the range of heating rates used in the paper the recrystallization of ferrite has small influence on the

structural composition of products and is not considered in this paper.

Model of the phase transformation during heating is also based on equation (1) with the coefficient $n = n_h$ and coefficient k defined as:

$$k_h = h_4 \exp\left[\frac{-h_5}{R(T+273)}\right] \tag{9}$$

Incubation time for the austenitic transformation is calculated from the equation:

$$\tau_h = \frac{h_1}{(T - \mathrm{Ae}_1)^{h_3}} \exp\left[\frac{h_2}{R(T+273)}\right] \tag{10}$$

Table 1. *Chemical composition of the investigated steels, wt %.*

steel	C	Mn	Si	Cr	Al	Nb	N
A	0.09	1.42	0.10	0.35	0.053	-	0.009
B	0.16	1.53	0.39	0.23	0.039	0.0132	0.006

Table 2. *Coefficients in the model determined from the dilatometric tests for the steel A*

n_h	h_1	h_2	h_3	h_4	h_5	n_f	a_1	a_2	p	q	n_p	p_1
1.21	32774	8.533	2.876	9.5×10^9	2.9×10^5	1.48	7.1	145.9	36.77	2.092	0.79	1397
p_2	p_3	k_p	n_b	b_0	b_1	b_2	b_3	b_4	b_5	b_6	m_1	m_2
67.7	3.47	1.85	0.461	683.3	24.2	24.9	1.7	0.006	0.187	0.519	428	2.902

Table 3. *Coefficients in the model determined from the dilatometric tests for the steel B*

n_h	h_1	h_2	h_3	h_4	h_5	n_f	a_1	a_2	p	q	n_p	p_1
0.23	1039	4.86	2.866	9636	7.94×10^4	1.62	8.4	170.9	72.6	2.68	0.835	21
p_2	p_3	k_p	n_b	b_0	b_1	b_2	b_3	b_4	b_5	b_6	m_1	m_2
0.37	0.006	0.276	1.86	722.7	29.03	26.34	1.68	2.1	2.81	2.6	409	21.4

Two DP steels were considered in the paper as a case studies. Chemical compositions of these steels are given in table 1. Main difference between Steel A und B is the carbon content, so different strength levels are adjustable (Steel A DP600; Steel B DP780). Coefficients in equations (1)-(10) for the investigated steels were identified on the basis of dilatometric tests and inverse algorithm described by Pietrzyk and Kuziak (2012). The values of these coefficients are given in table 2 and table 3. The model with identified coefficients was used in the present work to simulate continuous annealing of strips made of those two steels.

The phase transformations model based on equations (1) – (10) was incorporated into the user friendly computer system that was developed within the present work and was used as a support for fast and efficient design of various thermal cycles of continuous annealing.

3. CONTINUOUS ANNEALING

Typical thermal cycles for the continuous annealing are shown in figure 1. Two distinct cases of the annealing are presented in the figure. Both cases begin with heating with the rate dependent on the expected microstructure. Usually it is a moderate heating rate around 3°C/s. Static recrystallization of the ferrite occurs first in the deformed material. When temperature exceeds A_{c1} transformation of ferritic-pearlitic microstructure into austenite begins. Starting from this point the two cases are distinguished in figure 1. The intercritical thermal cycle of the continuous annealing is represented by triangular symbols in figure 1. In the intercritical region between temperatures A_{c1} and A_{c3} the isothermal holding or very slow heating with the rate of about 0.25°C/s is applied, generally for not longer than 40-60 s. A two-phase microstructure of ferrite and austenite is obtained. Continuous annealing with the maximum temperature exceeding A_{c3} can also be used. If it is the case, the whole ferrite is transformed into austenite after heating. This thermal cycles is represented by diamond symbols in figure 1. Cooling process begins next and it is usually composed of fast/slow and fast cooling periods and it can be similar for the two distinguished annealing cycles. After the first two periods of cooling, part of the austenite transforms back to ferrite. In the last period of quenching any remaining austenite is expected to transform to martensite, resulting in the

characteristic ferrite/martensite dual phase steel microstructure. See (Pietrzyk et al., 2014) for more details concerning investigation of various thermal cycles in the continuous annealing.

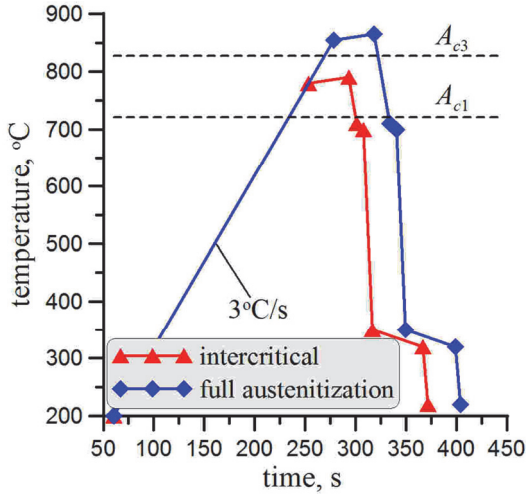

Fig. 1. *Typical thermal cycles for the continuous annealing.*

mon.MVC module, Model-View-Controller programming pattern was implemented to separate front-end from application logic. Graphical user interface (GUI), which makes the system user friendly, is based on Windows Forms technology. That is why some required abstract classes were implemented inside modules with names with Forms suffixes. This approach allows to adjust modules to the new front-end without changing these modules. *Common.Plotting* module provides results visualization tools that are useful for practical assessment of the designed thermal cycle. The output simulation data are stored inside local database created with the SqLite library and are easily accessible for visualization purposes. To improve working with the designed database, the NHibernate technology was used. Additionally *Common.NHibernate.Mapping* module was created to facilitate managing of database-objects.

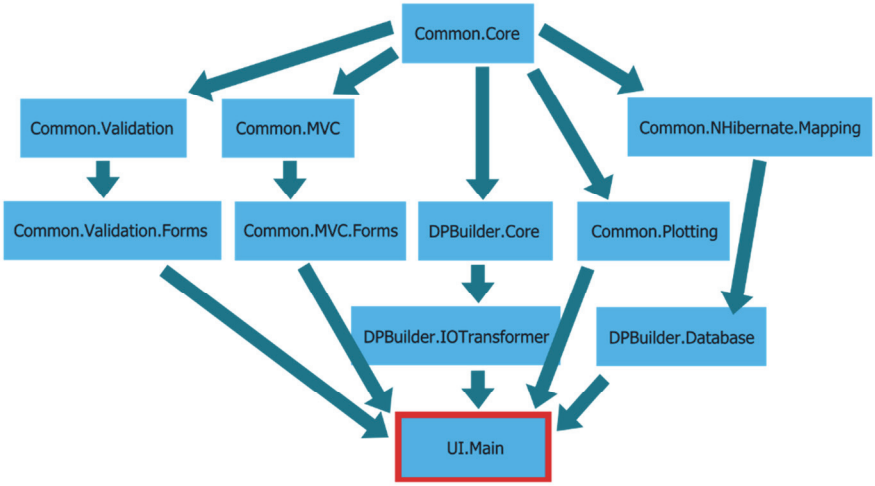

Fig. 2. *Dependence diagram for modules of the developed DP_builder software.*

4. COMPUTER SYSTEM

The developed user friendly software called *DP_builder* was created using the Microsoft .NET framework with C# programing language. Developed software can be used to design thermal cycle of DP steels as well as other AHSS steels. The system is divided into several major components, which are presented in figure 2.

The basic module in the system is called *Common.core*. This module stores all universal and common functionalities, which are necessary to link all libraries with common data types. *Common.Validation* module keeps logic, which is responsible for a proper data validation. Inside *Common.MVC* module, Model-View-Controller programming pattern was implemented to separate front-end from application logic. Graphical user interface (GUI), which makes the system user friendly, is based on Windows Forms technology. That is why some required abstract classes were implemented inside modules with names with Forms suffixes. This approach allows to adjust modules to the new front-end without changing these modules. *Common.Plotting* module provides results visualization tools that are useful for practical assessment of the designed thermal cycle. The output simulation data are stored inside local database created with the SqLite library and are easily accessible for visualization purposes. To improve working with the designed database, the NHibernate technology was used. Additionally *Common.NHibernate.Mapping* module was created to facilitate managing of database-objects.

Developed software consists of two parts, solver and managing GUI application. To provide communication between two applications, *DPBuilder.IOTransformer* module was developed. It is based on redirection and managing between Input/Output (IO) streams and files. All these modules are used by *UI.Main* module, which runs and joins them together. The diagram of developed database that stores both input and output data is presented in figure 3. Description of the software capabilities is presented in the following part of the paper.

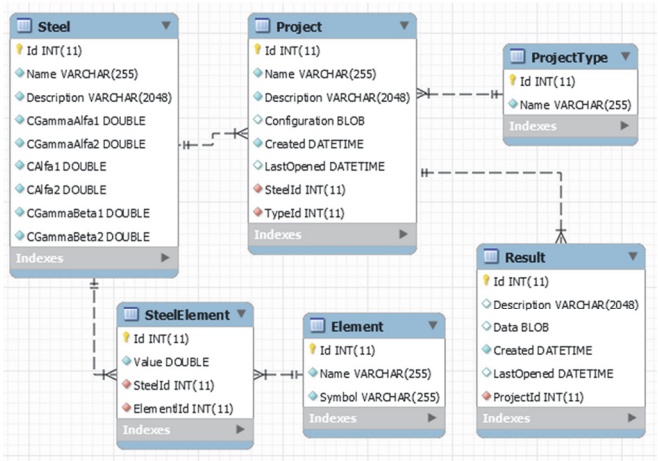

Fig. 3. *Database diagram with relations between tables.*

The main functionalities of the system compose simulation of phase transformations during thermal cycles and application of the optimization techniques to design the best technological variant. To reach these goals the system consists of a set of modules, which perform various functions:

– GUI (Graphical User Interface) layer, which allows to use application in an intuitive manner, controls correctness of the introduced data and presents obtained results (figure 4). GUI makes the software easily accessible and efficient.

Fig. 4. *Main window of the developed DP_builder software.*

– Database implemented with SQLite library. The database is used to store steels and projects data in an efficient way. It also stores material and technological data for all previously analysed cases.

– Console-based solver based on models presented in Chapter 2. The solver performs all simulations of phase transformation.

– Plotting and plot exporting libraries, which are used for visualization purposes.

The software is an easy to use application, which performs a complex set of actions such as:

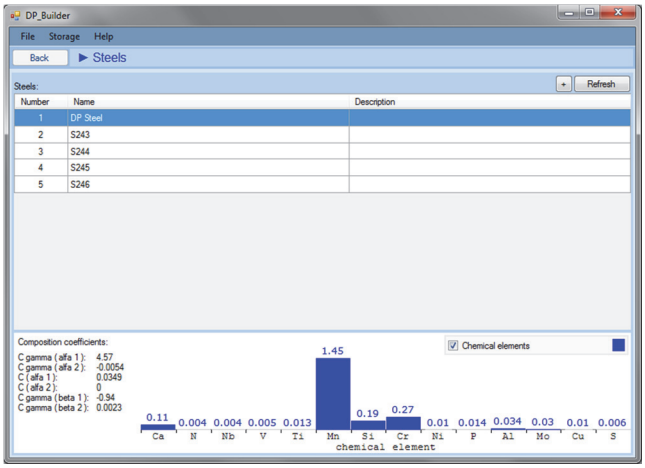

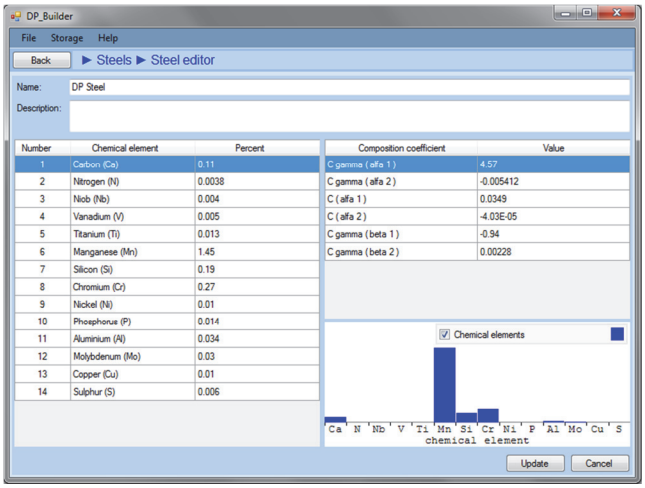

Fig. 5. *Window designed for creation and storage of steel parameters.*

– Creation and storage of steel parameters (figure 5).

Creation, storage and management of projects (figure 6). It allows to select which thermal cycles should be optimized and select solution space ranges of the investigated parameters.

– Simulation or optimization of continuous annealing processes, which can be performed in two modes. In the verification mode, which is used before permanent parameters change, and in recalculation mode to update results in the data base (figure 7). During optimisation it is possible to control process by monitoring error value with thermal cycles curve shape or breaking process and then setting a new configuration.

– Visualisation of results and comparing them with results obtained from other projects (figure 8).

– Export of stored results in the form of diagrams and text files (figure 9).

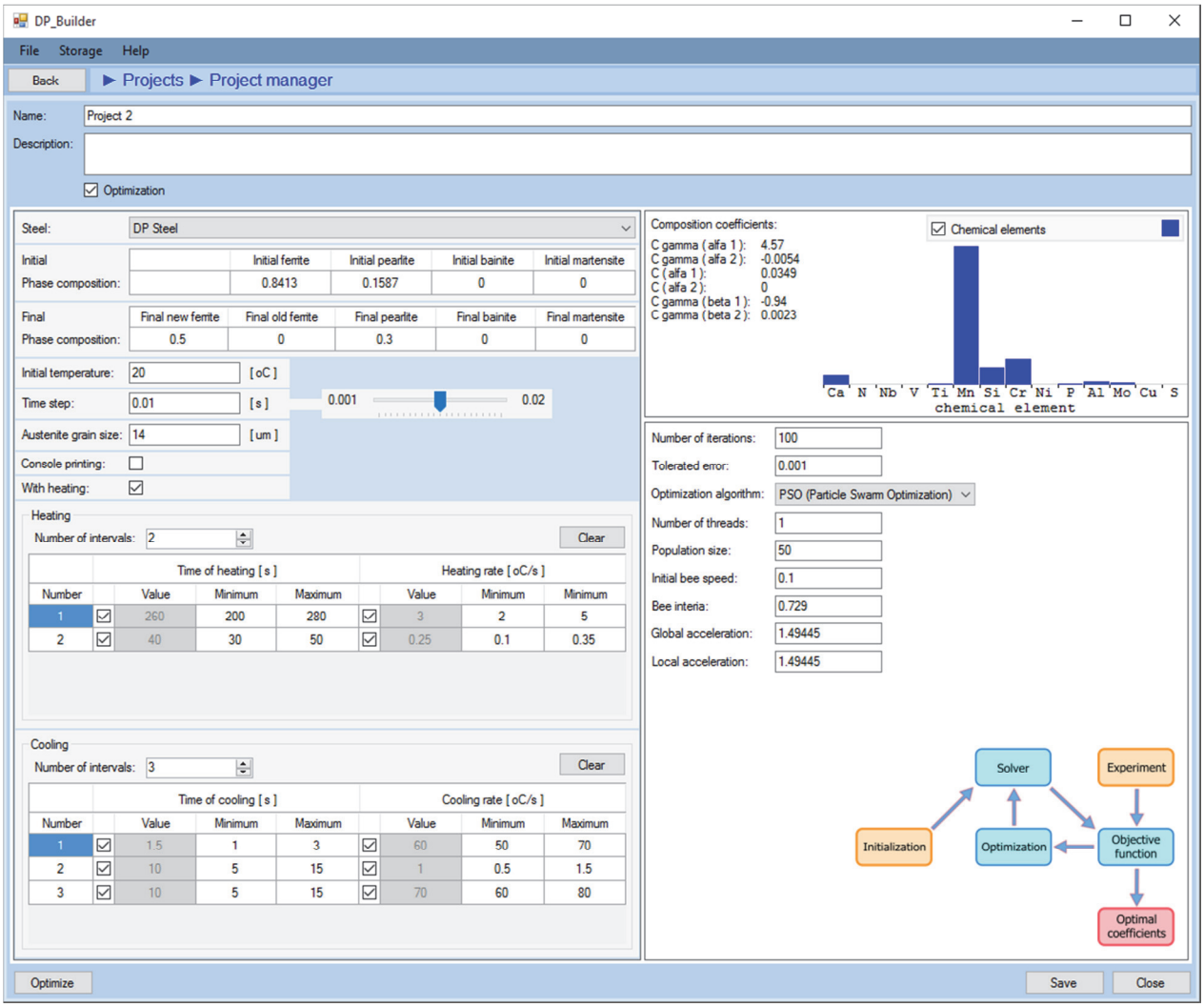

Fig. 6. *Window designed for creation, storage and management of projects in two variants: direct project configuration or thermal cycles optimisation project.*

In the designed system, the user controls the following parameters:

- phase composition, which includes initial content of ferrite, pearlite, bainite and martensite in the microstructure after cold rolling,
- initial temperature of the process,
- time step of the simulation,
- selection of thermal cycles for heating and cooling phases.
- Examples of practical applications of the developed software to design continuous annealing cycles are presented in the following part of the paper.

5. CASE STUDIES

Selected results of simulations of the continuous annealing performed using the developed computer system are presented below.

5.1. Simulation of laboratory tests

Developed model of phase transformations was validated in simulations of thermal cycles used in physical simulations performed on the dilatometer type DIL805. Tubular samples with the dimensions of $\phi 4 \times \phi 2 \times 5$ mm were used in the dilatometric tests. All tests were performed for steel A in table 1. Thermal cycles, which were investigated, are presented in figure 10. In all these cycles heating was performed with the rate of 3^{o}C/s. Three maximum temperatures were used: 790^{o}C in the cycle L1, 830^{o}C in the cycle L2 and 920^{o}C in the cycle L3. When maximum temperature of the cycle was reached cooling with different rates was performed, as shown schematically in figure 10a for the cycle L1 only. Eight different cooling rates between 1^{o}C/s and 300^{o}C/s were applied. The same cooling rates were applied in cycles L2 and L3, what is not shown in figure 10b to avoid making the figure not clear. All the tests were

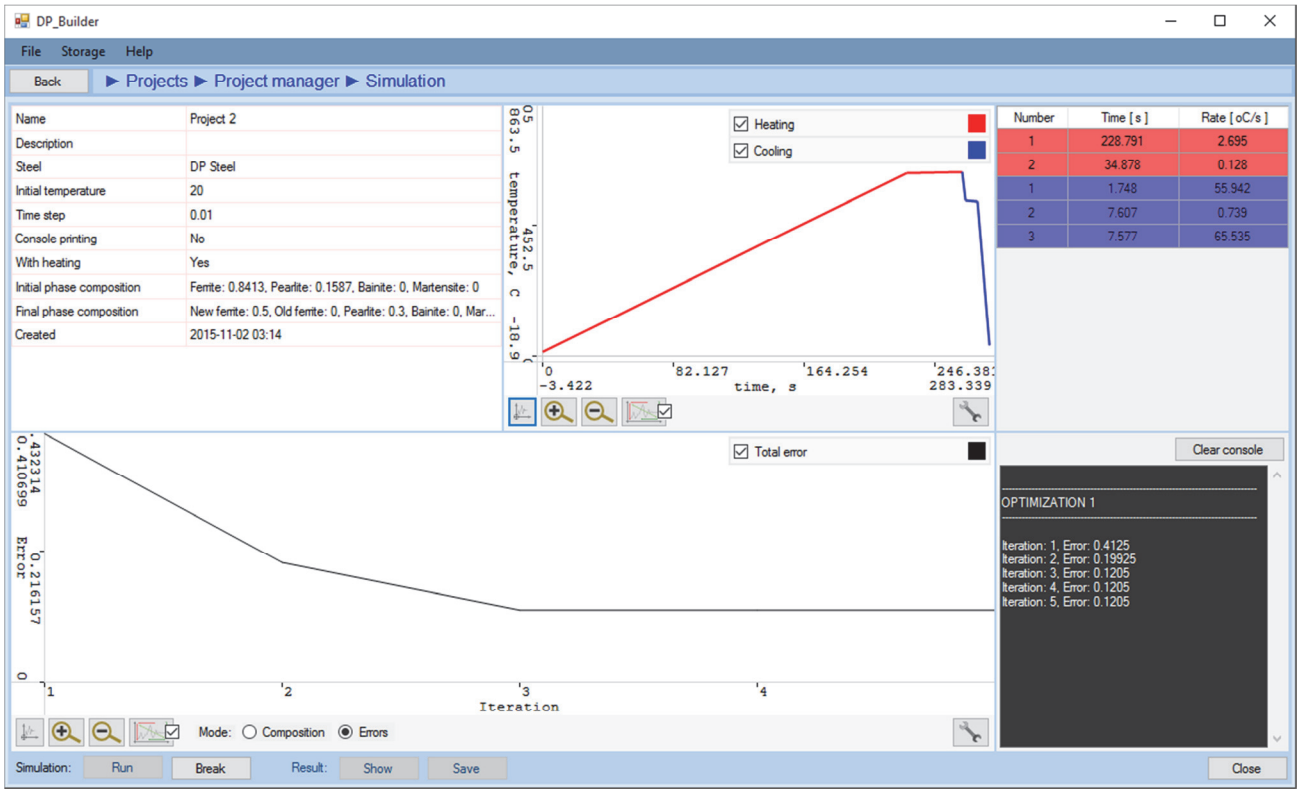

Fig. 7. *Optimisation preview window.*

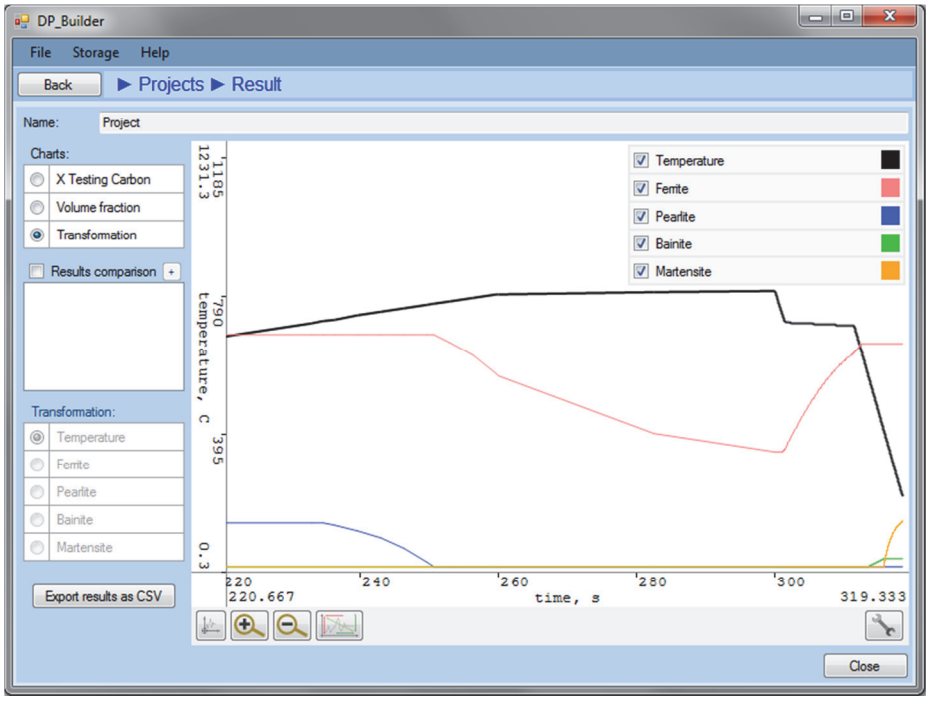

Fig. 8. *Visualization window.*

repeated twice. In the second set of experiments marked L4 – L6, the sample was maintained at the maximum temperature of the cycle for 20 s (figure 10b). Start and end temperatures of transformations and volume fractions of phases at the room temperature were measured in the experiments and were used for verification of the phase transformation model. Micrographs were made after each test and were used for evaluation of the phase compositions of samples. Typical microstructures for all tests with the cooling rate of 40°C/s are shown in figure 11. Since predictions of the model for the tests L3 and L6 were identical, results for L6 are not presented in the paper.

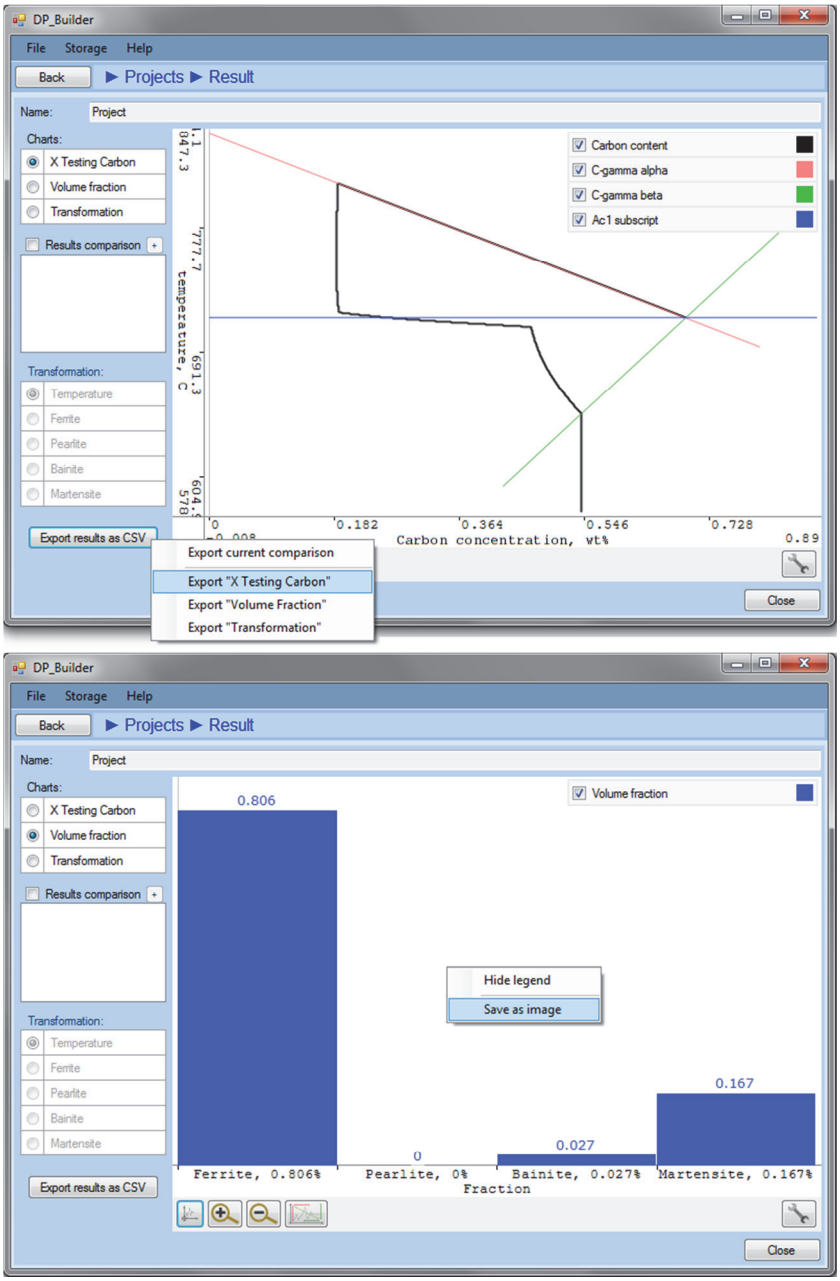

Fig. 9. Window designed for exporting of obtained results.

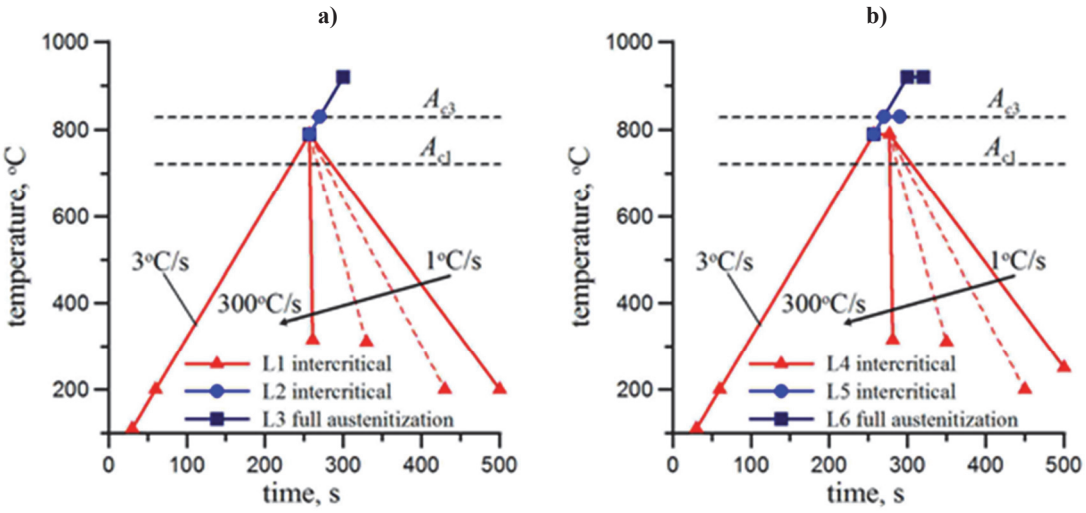

Fig. 10. Investigated laboratory thermal cycles without maintaining the sample at the maximum temperature (a) and with maintaining the sample at the maximum temperature for 20 s (b).

Calculated start and end temperatures of phase transformation for the cycle L1 are compared with the measured ones in figure 12 and good agreement was obtained. Kinetics of transformations during the cycles L2 – L5 are shown for the two representative cooling rates, for 1°C/s in figure 13 and for 40°C/s in figure 14. Volume fraction of the austenite was evaluated experimentally, as well, but quantitative analysis of the phase composition was difficult and the experimental results have to be treated as estimation only. In the tests with the maximum temperature of the cycle equal 790°C (L1 and L4) quantitative estimation of phase volume fractions was not possible. Similar situation was with the evaluation of the austenite volume fraction after heating in the tests L4 and L5.

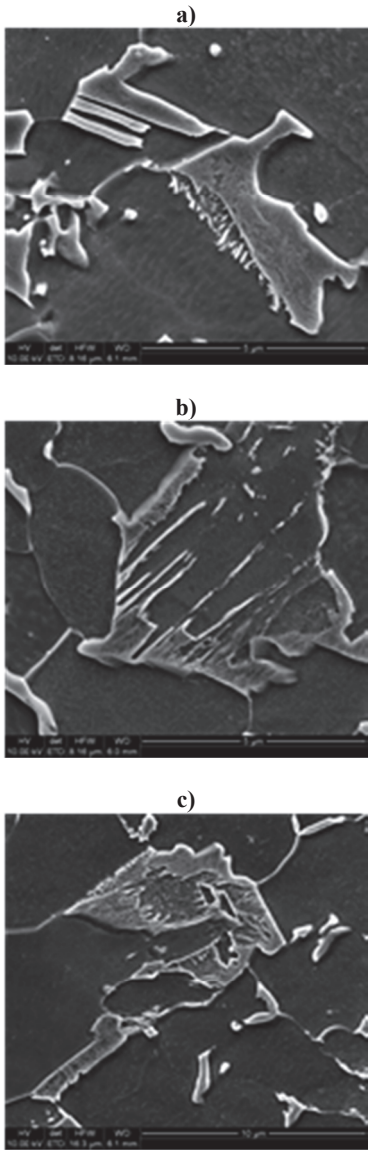

Fig. 11. Microstructures for the tests L4 (a), L5 (b) and L6 (c) for the cooling rate of 40°C/s. Steel A

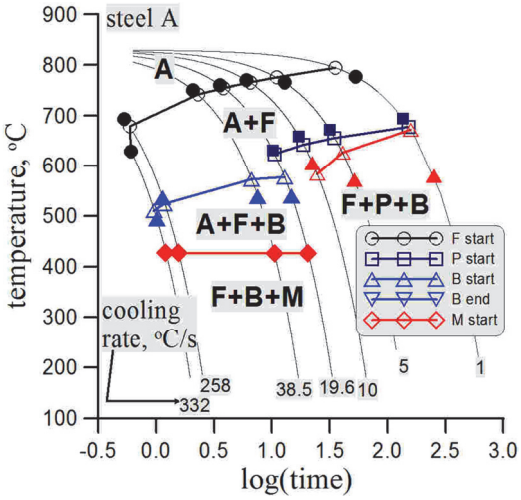

Fig. 12. Comparison of the predictions of the optimized model (coefficients in table 2) with measurements for the transformations start and end temperatures. Steel A

The volume fractions of phases were calculated by the model for all the tests and results are compared below. Volume fraction of the austenite after heating is presented in figure 15. It is seen in the figure that the model properly predicted amount of the austenite in the tests, where measurement was possible. Figure 15 shows results of calculations of volume fractions of phases in the tests L1 and L4, in which experimental quantitative evaluation was not possible. It is seen that maintaining the sample in the test L4 for 20 s at the maximum temperature of the cycle (790°C) resulted in an increase of the volume fraction of the austenite after heating and, in consequence, led to an increase of the volume fraction of the martensite after cooling.

Comparison of measured and calculated volume fractions of phases in the tests L2, L3 and L5 is shown in figure 17. The agreement between measurements and calculations is not very good and some discrepancies between measurements and predictions are observed. But it should be kept in mind that quantitative measurement of volume fractions in some tests was very difficult and experimental results have to be treated as estimations of the volume fractions.

Recapitulating this part of the work it could be concluded that numerical simulations of the laboratory tests confirmed good predictive capabilities of the developed model. Model predictions describe qualitatively very well kinetics of transformations and volume fractions of phases as functions of the annealing process parameters. Quantitative agreement between measurements and predictions is reasonable, having in mind difficulties with quantitative

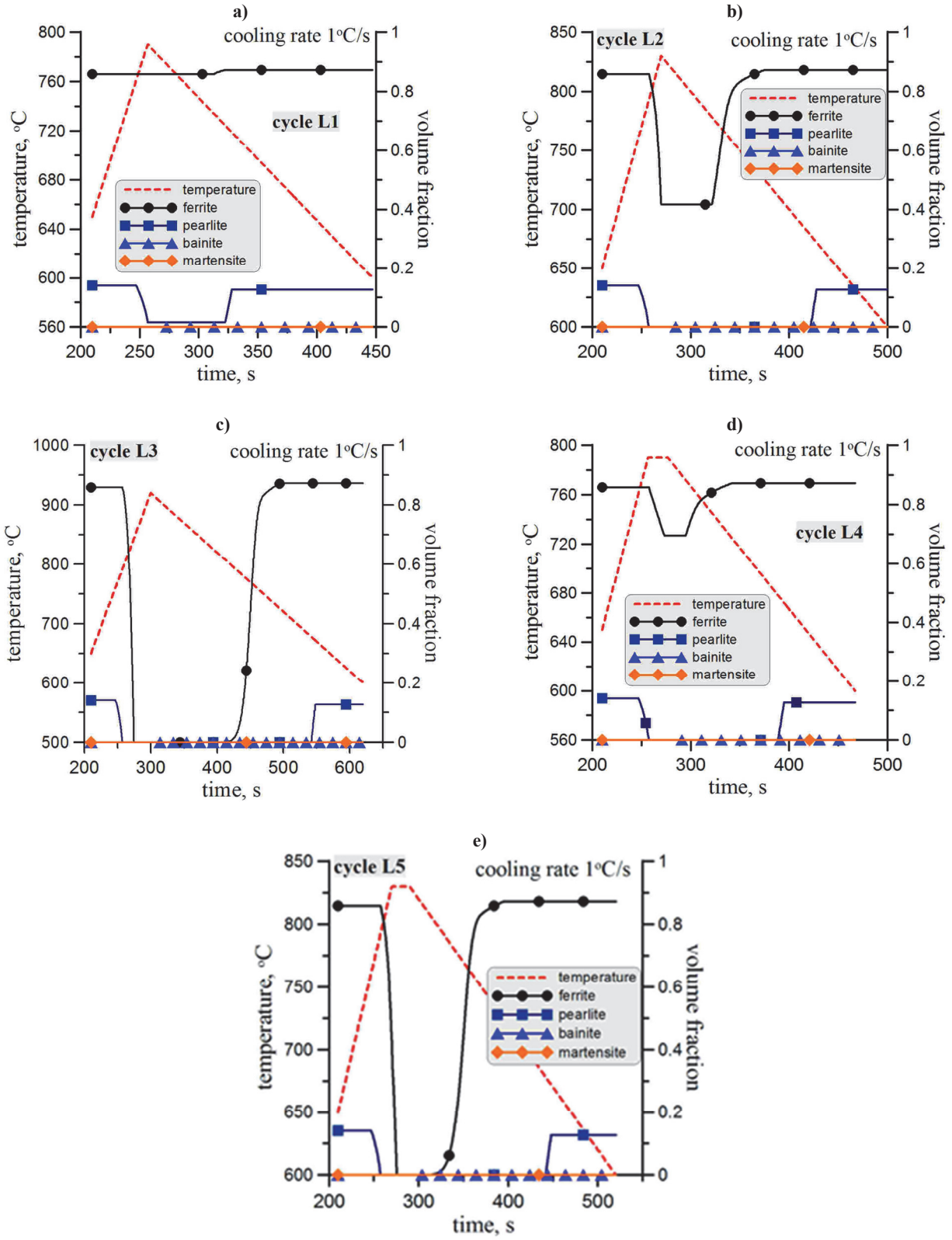

Fig. 13. *Kinetics of phase transformation during annealing cycles shown in Fig. 10; cooling rate 1°C/s (meaning of the symbols is the same in all plots). Steel A*

evaluation of the microstructure in the experiments. All these observations permit using the model in the system *DP_builder* for the optimization of the continuous annealing process.

5.1. Simulation of industrial tests

Simulation of the industrial annealing cycles for the steel B was performed next. Thermal cycles, which were investigated, are presented in figure 18. In all these cycles purely austenitic microstructure

was obtained after heating. Calculated by the system kinetics of phase transformation during cooling according to these four cycles is shown in figure 19. Calculations were stopped when the whole austenite was transformed into the low temperature phases.

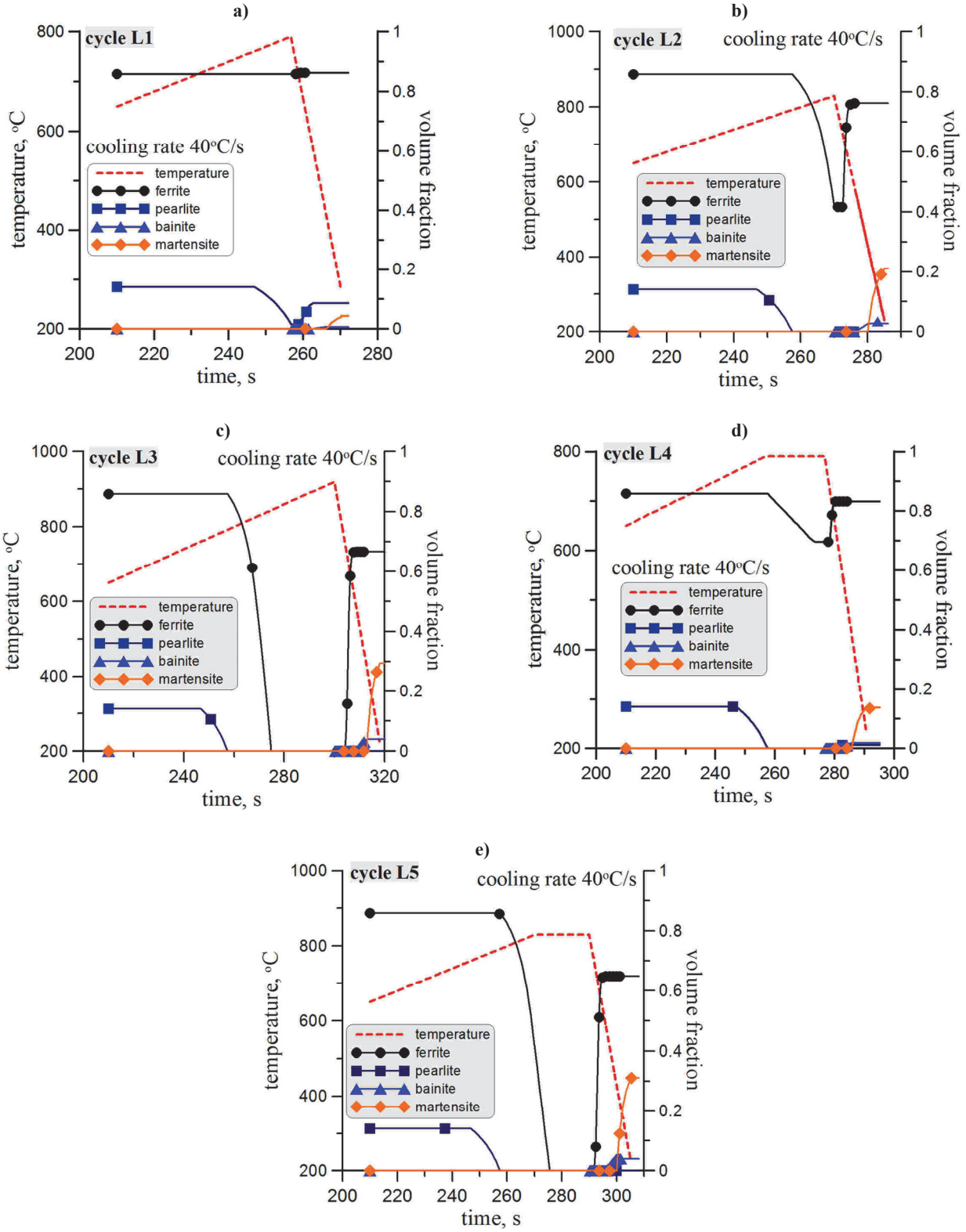

Fig. 14. *Kinetics of phase transformation during annealing cycles shown in figure 10; cooling rate 40°C/s (meaning of the symbols is the same in all plots). Steel A*

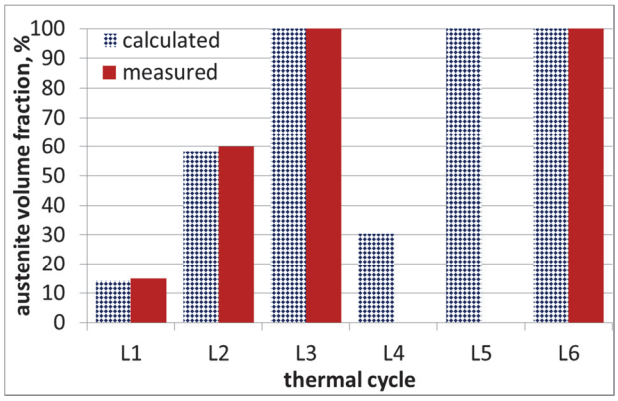

Fig. 15. Measured and calculated volume fraction of the austenite after heating.

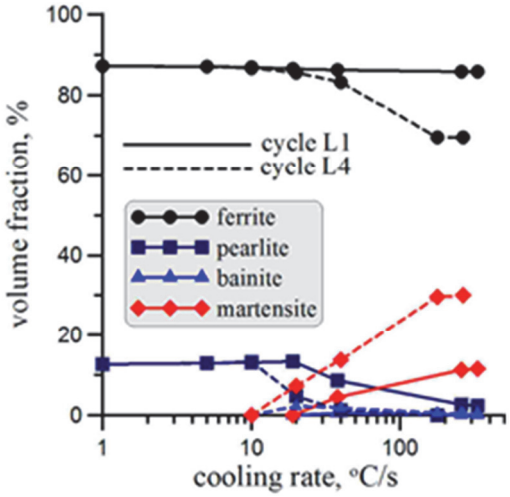

Fig. 16. Calculated volume fraction of phases in the tests L1 and L4.

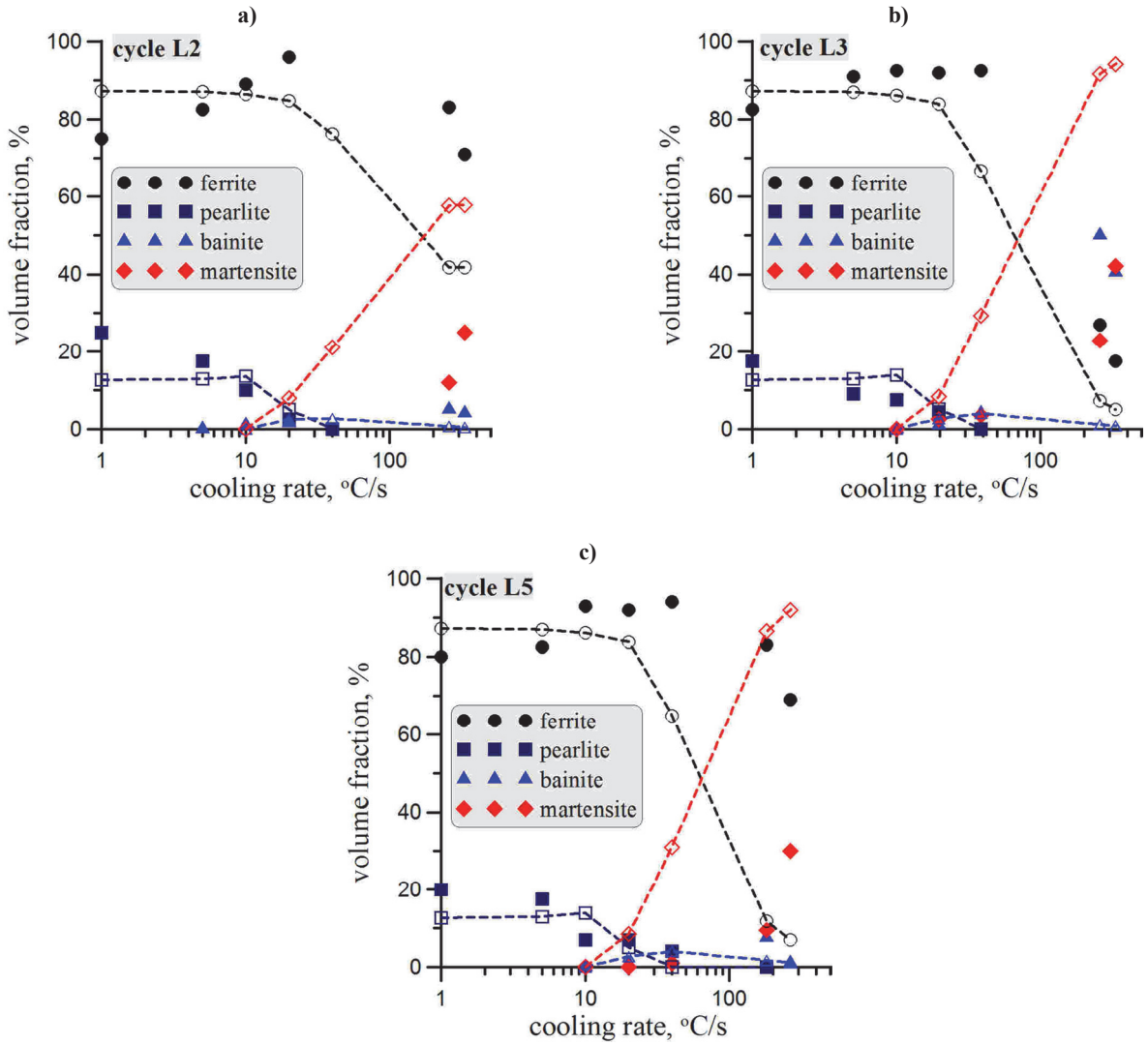

Fig. 17. Comparison of measured (full symbols) and calculated (open symbols with dashed lines) volume fractions of phases in the tests L2, L3 and L 5. Steel A

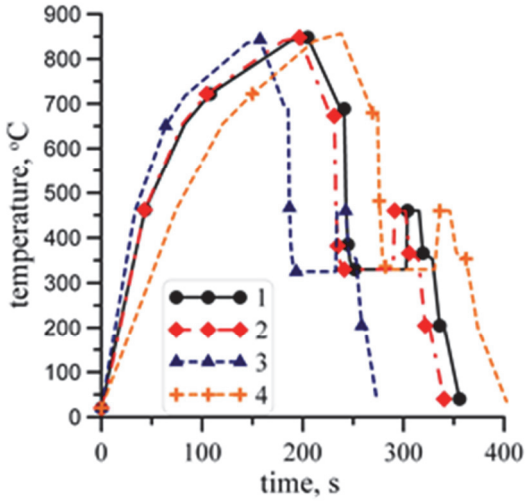

Fig. 18. Thermal cycles investigated for the steel B.

well. However, volume fractions of bainite and martensite differed. The maximum volume fraction of martensite was obtained for the cycle 3.

Numerical tests performed using the developed computer system *DP_builder* have shown that the phase transformation model presented in chapter 2 has a capability to describe process of continuous annealing of the investigated steel with good accuracy. Model supplies information concerning volume fractions of phases and changes of the average carbon concentration in the austenite as a function of parameters of the annealing thermal cycle.

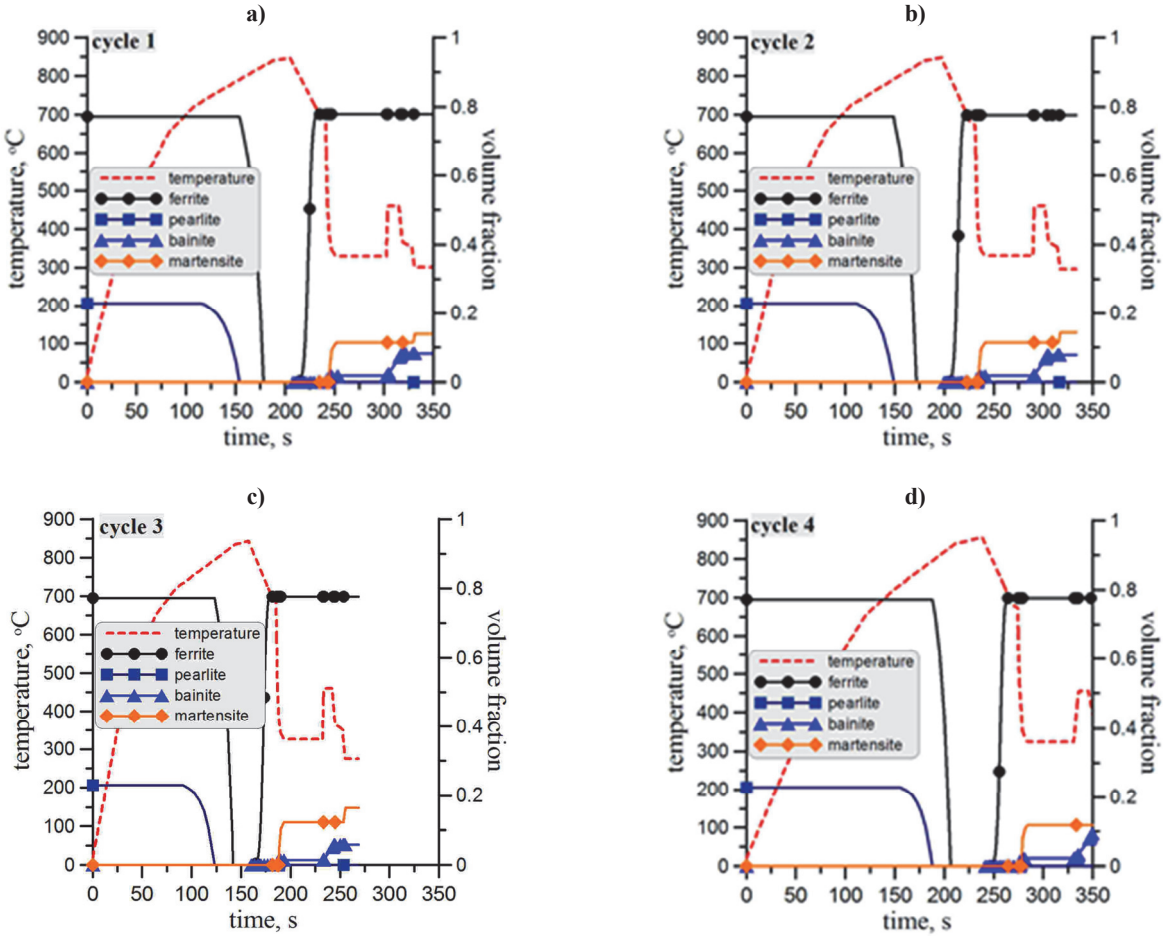

Fig. 19. Kinetics of phase transformation during cooling according to the annealing cycles shown in Fig. 18. Steel B

Calculated changes of the average carbon concentration in the austenite are shown in figure 20. Volume fractions of the ferrite, bainite and martensite are presented in figure 21. Analysis of all results shows that similar volume fraction of ferrite was predicted for all four cycles. It means that the total volume fraction of hard constituents was similar, as

7. CONCLUSIONS

The system *DP_builder*, which allows design of the continuous annealing technology for the DP steels, was presented in the paper. The virtual model of the industrial annealing process is the main part of

the system. Beyond this, the following functionalities of the system should be pointed out:

1. Possibility to store data.
2. User-friendly interface.
3. Convenient visualization of data.
4. Capability to simulate phase transformation during complex thermal cycles.

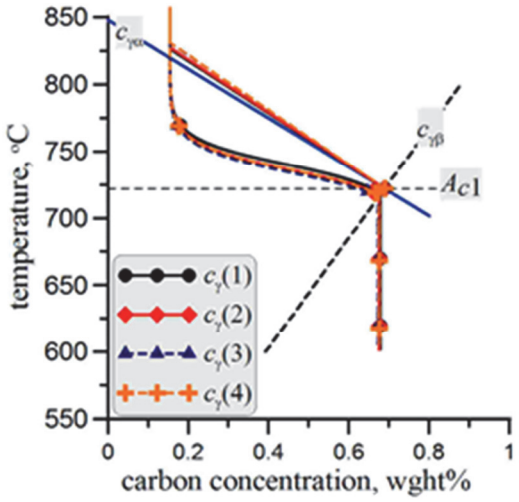

Fig. 20. *Changes of the average carbon concentration in the austenite during the four investigated thermal cycles for the steel B.*

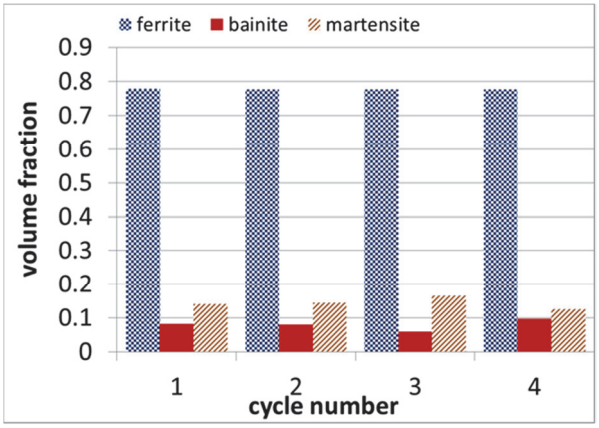

Fig. 21. *Volume fractions of phases calculated by the system for the four investigated thermal cycles for the steel B.*

The developed model, which is the basis of the system *DP_builder*, was validated by comparison its predictions with the results of the physical simulations of the continuous annealing and good agreement was obtained. The following conclusions were drawn on the basis of the performed numerical tests:

1. The model based on the JMAK equation with one coefficient described by the modified Gauss function gives good results as far as kinetics of transformations and volume fraction of phases have to be calculated.
2. This model is simple, easy for identification and reasonably accurate. Using the model in simulations of the continuous annealing is advised. Additivity rule has to be applied.
3. Regarding accuracy of the model in the predictions of temperatures for transformations, good agreement was obtained for all transformations. Some discrepancies were rather due to lack of consistency in the experimental data.

The system *DP_builder* can support the design of the best thermal cycle, which should be applied in the continuous annealing line to obtain the required phase composition of the DP steel.

ACKNOWLEDGEMENTS

The research leading to these results has received funding from the European Community Research Fund for Coal and Steel (RFCS) under grant agreement no. RFSR-CT-2011-00014. Finite Element calculations were realized at the ACK CYFRONET AGH MNiSW/IBM_BC_HS21/AGH/075/2010. Financial assistance of the MNiSzW, project no. SPB W75/FBWiS/2012, is also acknowledged.

REFERENCES

Avrami, M., 1939, Kinetics of Phase Change. I. General Theory, *J. Chem. Phys*., 7, 1103-1112.

Donnay, B., Herman, J.C., Leroy, V., Lotter, U., Grossterlinden, R., Pircher, H., Micro-structure evolution of C-Mn steels in the hot deformation process: the STRIPCAM model, *Proc. 2nd Conf. Modelling of Metal Rolling Processes*, eds, Beynon, J.H., Ingham, P., Teichert, H., Waterson, K., London, 1996, 23-35.

Hofmann, H., Mattissen, D., Schaumann, T.W., 2000, Advanced cold rolled steels for automotive applications, *Steel Research International*, 80, 22-28.

Koistinen, D.P., Marburger, R.E., 1959, A general equation prescribing the extent of the austenite-martensite transformation in pure iron-carbon alloys and plain carbon steels, *Acta Metallurgica*, 7, 59-69.

Matlock, D.K., Krauss, G., Speer, J.G., 2005, New microalloyed steel applications for the automotive sector, *Materials Science Forum*, 500-501, 87-96.

Matlock, D.K., Speer, J.G., 2009, *Third generation of AHSS: Microstructure design concepts*, Springer, 185-205.

Pernach, M., Kuziak, R., Pietrzyk, M., 2013, Problem doboru najlepszego modelu dla symulacji cyklu wytwarzania blachy ze stali DP, *Rudy i Metale Nieżelazne*, 58, 714-719 (in Polish).

Pietrzyk, M., Kuziak, R., Radwański, K., Szeliga, D., 2014, Physical and numerical simulation of the continuous annealing of DP steel strips, *Steel Research International*, 84, 99-111.

Pietrzyk, M., Kuziak, R., 2012, Modelling phase transformations in steel, *Microstructure evolution in metal form-*

ing processes, eds, Lin, J., Balint, D., Pietrzyk, M., Woodhead Publishing, Oxford, 145-179.

Suwanpinij, P., Togobytska, N., Prahl, U., Weiss, W., Hoemberg, D., Bleck, W., 2010, Numerical cooling strategy design for hot rolled Dual Phase steel, *Steel Research International*, 81, 22-28.

Scheil, E., 1935, Anlaufzeit der Austenitumwandlung, *Archiv für Eissenhüttenwesen*, 12, 565-567.

DP_BUILDER – SYSTEM DO KOMPUTEROWEGO WPIERANIA PROJEKTOWANIA CYKLI DLA PROCESU CIĄGŁEGO WYŻARZANIA STALI TYPU DP

Streszczenie

Przedstawiona praca opisuje zaprojektowany i zbudowany system, dzięki któremu w prosty sposób można zaprojektować technologię ciągłego wyżarzania stali typu DP (Dual-Phase). W pierwszej części pracy opisano główny moduł systemu wykorzystujący modele przemian fazowych podczas nagrzewania i chłodzenia. Następnie opisano zasady działania, dostępne funkcjonalności oraz szczegóły implementacyjne prezentowanej aplikacji. Główna funkcjonalność systemu łączy w sobie symulację ewolucji mikrostruktury podczas cykli nagrzewania i chłodzenia oraz optymalizację połączoną z procesem projektowania cykli, co daje duża swobodę podczas konfiguracji. Dodatkową funkcjonalnością systemu jest zdolność do przechowywania informacji o materiałach i parametrach technologicznych wszystkich analizowanych do tej pory przypadkach. Aby aplikacja była przejrzysta i łatwa w użytku wyposażono ją również w graficzny interfejs użytkownika.

Received: May 22, 2015
Received in a revised form: September 12, 2015
Accepted: October 23, 2015